A Cost-Efficient Improved VLSI Architecture for Buffer-less Edge-Oriented Demosaicking

Priyanka .H.T
Mtech in VLSI&Embedded System
Dr. Ambedkar Institute of Technology,near Jnana Bharathi Campus
Bengaluru,Karnataka-560056 ,Indian

Dr. G.V. Jayaramaiah
Professor and Head
ECE Department.
Dr. Ambedkar Institute of Technology
Bengaluru, Karnataka-560056, indian.

Abstract—

Color filter array interpolation in addition spoken as demosaicking and 'debayering', is also an important technique for image reconstruction in digital still cameras. This paper presents an edge-oriented demosaicking technique and an inexpensive very-large-scale integration (VLSI) style for color interpolation. the planning uses easy operations (addition, subtraction, shift, and comparator) and nearest neighboring pixels to catch the color distinction and edges. There are no requirements of line buffering in the proposed; therefore, its hardware value is low by 90 percent. Our intensive experiments disclosed that the projected technique preserved edge options and exhibited superb qualitative analysis and visual quality performances. Compared with the previous VLSI implementations, the projected vogue achieved superior image qualities. The synthesis results disclosed that by exploitation Taiwan Semiconductor manufacturing Company zero.18-µm technology the projected style yields a process rate of roughly two hundred M samples per second.

Index Terms — **Color filter array (CFA) interpolation, demosaicking, pipeline architecture, very-large-scale integration (VLSI).**

I. INTRODUCTION

Digital pictures are comprised of data samples geared up in a two dimensional grid. These information samples are generally referred to as picture elements or pixels. The quantity of pixels in a photograph determines its resolution. The greater range of pixels an image has the greater data it could include and consequently the better it ought to symbolize the authentic data. In other words, all other things being equal, a high-resolution photo has higher quality than a low resolution one.

Camera lens area unit extensively utilized in client electronic merchandise, like digital cameras, mobile phones, action cameras, and tablets. A digital icon is generally composed of 3 channels (i.e. red, green, and blue), thus it needs 3 separate icon sensors for mensuration icon channel. To decrease prices, most camera manufacturers use one image detector and a color filter array (CFA) to report one among the 3 main channels at every pattern location. Thus, CFA interpolation, additionally considered demosaicking, and debayering, is needed to reconstruct a full-colour image. the foremost common CFA is that the Bayer CFA pattern [1] (Fig. 1). The **B**ayer array measures the inexperienced channel on a quincunx grid, and thus the crimson and blue channels on rectangular grids. Demosaicking or Color Filter Array (CFA) interpolation is a unique photograph interpolation drawback. Here, the photo size is constant however only a subset of the colour information is accessible at every pixel location. The missing statistics at each region needs to be estimated to obtain the entire shade image. Whereas spatial correlation is the only estimation groundwork for everyday picture interpolation, spectral correlation between the shade channels additionally comes into play for the demosaicing problem. Demosaicing algorithms need to take advantage of each of them to keep away from false shade artifacts that are closely associated with the demosaicing process.

In several wise applications, the demosaicking technique is enclosed within the photographic camera, consequently a fascinating demosaicking approach appropriate for fewer high-priced VLSI implementation is needed and also the hardware worth is incredibly vital. Generally, the value of VLSI implementation depends loosely on the desired reminiscence and procedure quality. However, the resolution of photographic camera pics extended from VGA (640X480) to presently 4K immoderate HD (4096X2160). the massive the image, the larger the road buffering is needed. Therefore, the desired line buffering can become the foremost essential issue of the hardware value.

Several lower-cost demosaicking methods are planned within the past few years. additive interpolation (BI) is that the best strategy for image reconstruction. The ultra-low-cost coloration demosaicking VLSI diagram was once planned with the help of Chen et al. The hardware value was once perceptibly reduced. The reconciling edge-enhanced interpolation (EECP) approach planned by Chen and Ma uses a side detector, AN aeolotropic weight model, and a filter-based compensator for decreasing memory needs and meliorative image quality. Chen AND river introduced an fully pipelined CFA interpolation set up (FPCD) that uses linear deviation compensation, instantly interpolated inexperienced coloration pixels, a boundary detector and a boundary mirror machine meliorative the exceptional of a reconstructed image. Shiau et al. planned AN area-efficient coloration demosaicking theme (ACDS) for VLSI structure that uses side statistics and inter-channel correlations. The VLSI design is economical once the resource-sharing and pipeline-scheduling ways are used. The reconstructed image quality of lower-cost methods is generally poor, and will in addition incorporate false colours, zipper effects, or both. Conversely, the higher-cost interpolation methods yield visually appealing pictures. several period functions embrace the demosaicking procedure within the end-user equipment; thus, the demand for a positive, lower-cost demosaicking approach that is appropriate for lower-cost VLSI implementation has magnified. Affordability may be a crucial thought once shopping for patron electronic product. For affordability, low fee is needed. This paper focuses on lower-cost demosaicking techniques, thanks to the actual fact of their simplicity and simple implementation with a VLSI circuit. Moreover, edge holding techniques ar wide utilized in several digital photograph process fields, appreciate image deinterlacing, image scaling, and exposure denoising then on. They used relevant shade knowledge to yield higher exposure quality or to stay faraway from image blur.

According to these basic ideas, a unique edge-oriented demosaicking approach (EODM) and associated VLSI structure for digital still cameras is bestowed. the desired line buffering of the planned sketch is four lines; thus, its hardware price is low. For a 768×512 eight-bit CFA take a glance at image, EODM needs four traces (768×4×8 bits); several superior ways buffer additional than eight lines. a number of them needed twenty-five strains for line buffering. In our style, storage was once ablated via larger than 90%; by utterly eliminating the buffers what is more, easy arithmetic operations, like adder, subtractor, shifter, and comparator were used.

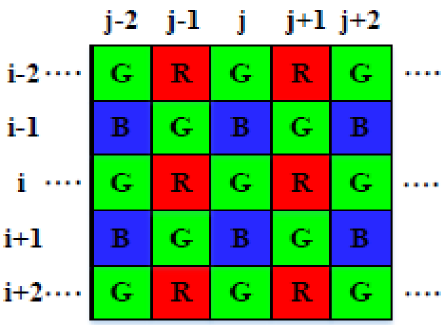

Figure1: Bayer CFA pixels

II. History of Demosaicking

Color photos require more than one data samples for every pixel as against grayscale images for which a pixel is represented through only one statistics sample. For the RGB image format, these records samples symbolize red, green, and blue channels. A traditional digital camera captures solely one of these channels at every pixel vicinage and also the different two desires to be estimated to generate the entire colour information. This technique is known as Color Filter Array (CFA) interpolation or demosaicking. Although many CFA patterns have been proposed over the years, the most regularly occurring one is the Bayer sample shown in Figure 1. Bayer pattern is an instance of pure RGB based totally CFA patterns. Some sample designs are comprised of elements that are mixtures of RGB colors such as the Hirakawa pattern as an important step in picture processing pipeline of digital cameras, demosaicing has been an vicinity of activity both in academia and industry. The easiest strategy to the demosaicing problem is to deal with color channels separately and fill in lacking pixels in every channel the use of a spatially invariant interpolation technique like bilinear or bicubic interpolation. While such a strategy works high-quality in homogenous areas, it leads to coloration artifacts and decrease resolution in regions with texture and facet structures. Obtaining higher demosaicing overall performance is viable by using exploiting the correlation between colour channels. Spectral correlation can be modeled by means of both constant color ratio rule and regular coloration difference rule. The simple assumption is that shade ratio/difference is consistent over a nearby distance inside a given object. This assumption is in all likelihood to smash apart across boundaries; for that reason many demosaicing algorithms attempt to make use of it adaptively in one way or another.

Since Bayer CFA sample has twice as many green channel samples as crimson and blue ones, green channel suffers much less from aliasing and it is the natural selection as the beginning point for CFA interpolation process. In Glotzbach et al. proposed improving crimson and blue channel interpolation by means of adding high frequency factors extracted from green channel to purple and blue channels. In another, frequency area approach, Gunturk et al. used an alternating projections scheme based totally on sturdy inter-channel correlation in excessive frequency sub bands. Although the most important objective is to refine crimson and blue channels iteratively, the equal strategy can additionally enhance green channel interpolation earlier which in turn yields higher red and blue channel results. A more current technique makes several observations about color channel frequencies and suggests that filtering the CFA picture as a total instead of person coloration channels have to retain high frequency information better. To estimate luminance, the approach proposes a fixed 5 by 5 filter at inexperienced pixel locations and an adaptive filter for pink and blue pixel locations. Estimated full decision luminance is then used to complete the missing chrominance information. Edge-directed inexperienced channel interpolation has been proposed early on with number course choice rules. Several subsequent demosaicing algorithms made use of this idea. Authors of proposed the use of variance of color variations as a choice rule whereas Zhang et al. proposed system is making a tender decision to improve the interpolation performance of the authentic method. In this method, color variations along horizontal and vertical directions are treated as noisy observations of goal pixel colour distinction and they are blended optimally using Linear Minimum Mean square Error Estimation (LMMSE) framework. Paliy et al. similarly multiplied directional filtering proposed in through introducing scale adaptive filtering primarily based on linear polynomial approximation (LPA). Several techniques proposed performing interpolation in each horizontal and vertical directions and making a posteriori selection primarily based on some criteria. Hirakawa et al. compared local homogeneity of horizontal and vertical interpolation effects and Menon et al. used colour gradients over a nearby window to make the direction selection.

III. EXISTING SYSTEM

In several wise applications, the demosaicking procedure is enclosed within the camera, consequently an honest demosaicking methodology applicable for inexpensive VLSI implementation is required and in addition the hardware worth is extremely necessary. Generally, the worth of VLSI implementation depends upon totally on the desired memory and process quality. However, the resolution of camera images increased from VGA (640X480) to presently 4K extremist HD (4096X2160). the big the image, the higher the road buffering is needed. Therefore, the desired line buffering can become the foremost very important component of the hardware value. Since the mask size decides the traces of line buffering, we've a bent to require five traces because the margin to lower-cost techniques and higher-cost strategies. Hence, these demosaicking techniques are often categorized as either higher-cost interpolation strategies or lower value.

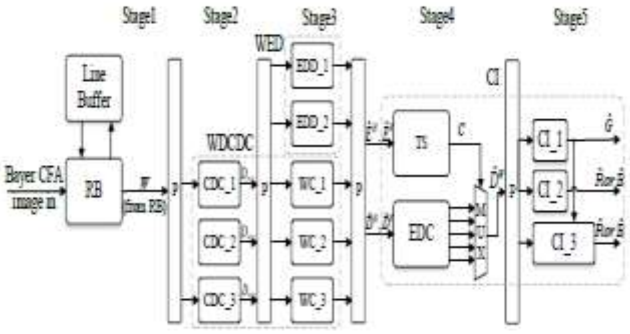

Figure 2. Block diagram of VLSI architecture of the EODM

IV. PROPOSED ALGORITHM

Ideal Interpolation Sampling of a continuous image f(x, y) yields endless repetitions of its non-stop spectrum F (z, h) in the Fourier domain. If these repetitions do no longer overlap which is almost by no means the case as natural pictures are now not band limited? The original picture f(x, y) can be reconstructed exactly from its discrete samples f (m, n); otherwise we examine the phenomenon of aliasing. The one-dimensional ''ideal'' interpolation is the multiplication with a rect function in the frequency domain and can be realized in the spatial area through a convolution with the sinc function. Kernel is band limited and, hence, is not space limited. It is especially of theoretical interest and not applied in practice.

Neighborhood issues it may be predicted that we get better estimates for the lacking pattern values by increasing the neighborhood of the pixel, on the other hand this increase is computationally expensive. There is, hence, a need to keep the interpolation filter kernel space-limited to a small measurement and also extract as an awful lot data from the neighborhood as possible. To this end, correlation between colour channels is used. 12 For RGB images, cross correlation between channels has been determined and observed to fluctuate between 0.25 and 0.99 with averages of 0.86 for red/green, 0.79 for red/blue, and 0.92 for green/blue cross correlations. Red and blue are perfectly correlated with the green over a small neighborhood and thus vary from green by only an offset. The same applies at a blue pixel location. The desire of the regional size in such a case is important. It is found that most implementations are designed with hardware implementation in thinking paying terrific attention to the need for pipelining, system latency, and throughput per clock cycle. The larger the neighborhood, subjected to the increase in the pipeline, the higher the latency and per chance lesser the throughput. This technique is proposed with the aid of Hamilton and Adams.

For CFA interpolation, the Bayer pattern was considered. The proposed EODM consists of four components, particularly

1. Weighting directional colour difference calculator (WDCDC).
2. Weighting area detector (WED).
3. G-plane interpolator (GI).
4. R-plane and B-plane interpolator (RI&BI).

The Figure 4 shown below illustrates the EODM design concept. The four components are described in the following sections

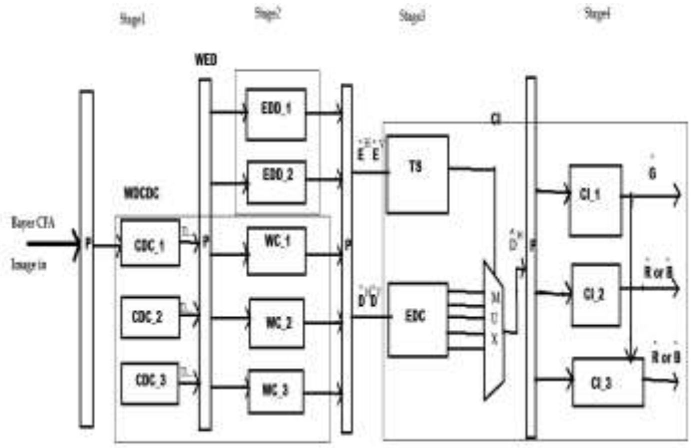

Figure 3. Block diagram of Proposed VLSI architecture of the EODM

Figure 3 displays the 2 stage pipeline structure of the WDCDC, within which P represents the pipeline registers. W represents the picture element values of the present mask of $P_{i,\ j}$. The WDCDC used to be composed of six small modules. The modules CDC_1, CDC_2, and CDC_3 have been used to calculate the directional shade difference values in Case 1, 2, and 3, respectively, Figure 7 shows a targeted implementation of CDC_1 if the output is $\boldsymbol{D}_{i,j}^{H_{OR}}$ as mentioned in equation 1. The modules WC_1, WC_2, and WC_3 had been used to generate the weighing directional shade differences. Figure 9 shows the unique implementation of WC_1

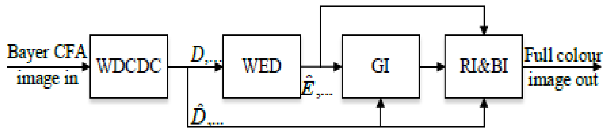

Figure 4: EODM dataflow

1. Weighting Directional Color Difference Calculator

For real-world pictures, the contrasts of G-R and G-B square measure notably flat over tiny regions; this property is fabulous for interpolation. Therefore, the interpolation of the R, G, and B channels uses G-R and G-B data. Assume that the component to be demosaicked is positioned at coordinate (i, j) and denoted as $P_{i,j}$ in keeping with the colour channel of $P_{i,j}$ the WDCDC will be divided in to 3 cases: Interpolating the inexperienced channel price of $P_{i,j}$ once the colour channel of $P_{i,j}$ is R channel or B channel.

(a) Interpolating the red or blue channel $P_{i,j}$ once the colour channel of $P_{i,j}$ is B channel or R channel severally.

(b) Interpolating the red or blue channel price of $P_{i,j}$ once the colour channel of $P_{i,j}$ is G channel.

In Case 1, if the colour channel of $P_{i,\ j}$ is R channel, the horizontal and vertical color variations are often calculated by using G-R data and denoted as $D_{i,j}^{HGR}$, and $D_{i,j}^{VGR}$, severally.

$$D_{i,j}^{H_{OR}} = (G_{i,j-1} + G_{i,j+1})/2 - (\widetilde{R}_{i,j-1} + \widetilde{R}_{i,j+1})/2, \quad (1)$$

$$D_{i,j}^{V_{OR}} = (G_{i-1,j} + G_{i+1,j})/2 - (\widetilde{R}_{i-1,j} + \widetilde{R}_{i+1,j})/2, \quad (2)$$

Where, H and V represent the horizontal and vertical directions, respectively.

$\widetilde{R}_{i,j-1}$, $\widetilde{R}_{i,j+1}$, $\widetilde{R}_{i-1,j}$, and $\widetilde{R}_{i+1,j}$, are the estimates obtained by averaging two directional neighbor pixels. For example, in (1) $\widetilde{R}_{i,j-1} = (\widetilde{R}_{i,j-2} + \widetilde{R}_{i,j})/2$.

To gain larger precise information on horizontal and vertical color variations, the planned technique utilized the distances between the closest eight neighboring pixels and also the middle pixel, and calculated the weighted average of the directional color variations. They are denoted as $\widehat{D}_{i,j}^{H_{OR}}$ and $\widehat{D}_{i,j}^{V_{OR}}$ .The equations are expressed as follows:

$$\widehat{D}_{i,j}^{H_{OR}} = \begin{bmatrix} D_{i-2,j-1}^{H_{OR}} & D_{i-2,j}^{H_{OR}} & D_{i-2,j+1}^{H_{OR}} \\ D_{i,j-1}^{H_{OR}} & D_{i,j}^{H_{OR}} & D_{i,j+1}^{H_{OR}} \\ D_{i+2,j-1}^{H_{OR}} & D_{i+2,j}^{H_{OR}} & D_{i+2,j+1}^{H_{OR}} \end{bmatrix} * W_D, \quad (3)$$

TABLE I
FIVE POSSIBLE VALUES OF *C* AND THEIR CORRESPONDING DIRECTIONS IN THE EODM.

Type	*C*	the chosen case
Normal Horizontal Edge	000	$if\ 4 \times \widehat{E}^{H_{OR}} \le \widehat{E}^{V_{OR}}$
Slight Horizontal Edge	001	$if\ 2 \times \widehat{E}^{H_{OR}} \le \widehat{E}^{V_{OR}} < 4 \times \widehat{E}^{H_{OR}}$
Normal Vertical Edge	010	$if\ 4 \times \widehat{E}^{V_{OR}} \le \widehat{E}^{H_{OR}}$
Slight Vertical Edge	011	$if\ 2 \times \widehat{E}^{V_{OR}} \le \widehat{E}^{H_{OR}} < 4 \times \widehat{E}^{V_{OR}}$
No Edge	100	*Othervise*

Table 1: Five Possible values of C and their Corresponding

$$\widehat{D}_{i,j}^{V_{OR}} = \begin{bmatrix} D_{i-1,j-2}^{V_{OR}} & D_{i-1,j}^{V_{OR}} & D_{i-1,j+2}^{V_{OR}} \\ D_{i,j-2}^{V_{OR}} & D_{i,j}^{V_{OR}} & D_{i,j+2}^{V_{OR}} \\ D_{i+1,j-2}^{V} & D_{i+1,j}^{V_{OR}} & D_{i+1,j+2}^{V_{OR}} \end{bmatrix} * W_D, \quad (4)$$

$$W_D = \frac{1}{16}\begin{bmatrix} 1 & 2 & 1 \\ 2 & 4 & 2 \\ 1 & 2 & 1 \end{bmatrix} \quad (5)$$

The equations for the weight directional color variations in different cases are almost like the equations (1)–(5). Then the two interpolators (GI and RI& BI) used these two records to interpolate the missing channels.

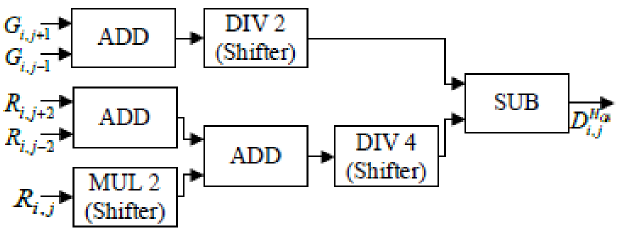

Figure5: CDC_1 ($D_{i,j}^{H_{OR}}$) module architecture

2) Weighting Edge Detector

For additional fascinating image quality, a weight edge find or module was once used to detect an edge. The WED makes use of the results of the previous step to accumulate horizontal and vertical edges. For a further precise edge, the weighted average of the edges of the closest 2 neighboring constituents and also the centre pixel won't to be thought of. In Case 1, if the color channel of pixel $P_{i,j}$ is R, the horizontal and vertical edges are denoted as $E_{i,j}^{H_{OR}}$ and $E_{i,j}^{V_{OR}}$, the weighted edges are denoted as $\widehat{E}_{i,j}^{H_{OR}}$ and $\widehat{E}_{i,j}^{V_{OR}}$ respectively. The equations are expressed as follows:

$$E_{i,j}^{H_{OR}} = |D_{i,j-1}^{H_{OR}} - D_{i,j+1}^{H_{OR}}|, \quad (6)$$

$$E_{i,j}^{V_{OR}} = |D_{i-1,j}^{V_{OR}} - D_{i+1,j}^{V_{OR}}|, \quad (7)$$

$$\widehat{E}^{H_{OR}} = \begin{bmatrix} E_{i-2,j}^{H_{OR}} \\ E_{i,j}^{H_{OR}} \\ E_{i+2,j}^{H_{OR}} \end{bmatrix} * W_E, \quad (8)$$

$$\widehat{E}^{V_{OR}} = [E_{i,j-2}^{V_{OR}} \quad E_{i,j}^{V_{OR}} \quad E_{i,j+2}^{V_{OR}}] * W_E, \quad (9)$$

$$W_E = \frac{1}{4}[1 \quad 2 \quad 1]. \quad (10)$$

The equations of the weighted edges in different cases area unit like (6)–(10). For interpolating the missing color channel, the weighted color variations and weighted edges were thought-about. GI is employed for interpolating the inexperienced channel just in case one. RI&BI is used for interpolating the red and blue channel just in case a pair of and three. they're described within the following sections.

Figure 3 displays the pipeline design of the WED, that was composed of two little modules. The modules from EDD_1 to EDD_2 were wont to calculate the directional variations, as mentioned within the Figure6 depicts the elaborated implementation of EDD_1 if the output is as mentioned in equation (8). The unit |SUB| is employed to output absolutely the value of distinction of two inputs. The WC module was wont to calculate the weighted edge.

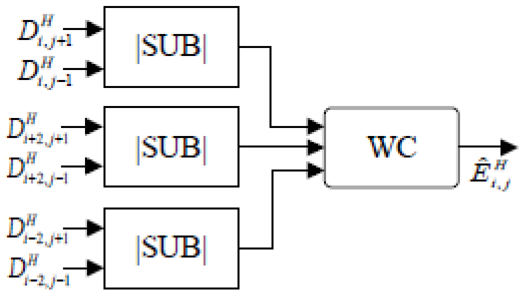

Figure 6: EDD_1 $\widehat{E}_{i,j}^{H}$ module architecture

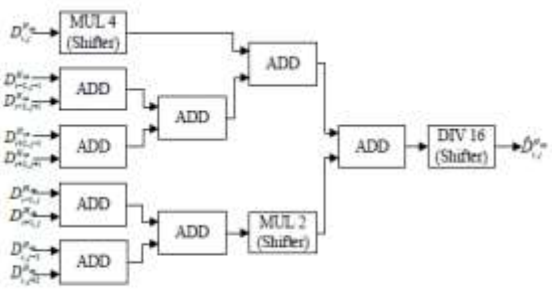

Figure7: WC_1 module architecture

C) G-plane Interpolator

In case 1, if the color channel of $P_{i,j}$ is R, the weighted color differences, $\widehat{D}_{i,j}^{Hgr}$ and ,$\widehat{D}_{i,j}^{Vgr}$ and weighted edges, $\widehat{E}^{Hgr}$ **and** $\widehat{E}^{Vgr}$ were considered for interpolating the missing green channel in the R channel. The degree of ratio between $\widehat{E}$ ^{Hgr} **and** $\widehat{E}$ ^{Vgr} were determined. The five sorts are indentified as traditional horizontal edge, moderate horizontal space , traditional vertical edge kind, slight vertical edge kind, and no edge. within the traditional horizontal side kind, only the horizontal statistics was wont to interpolate the lacking constituent, which may be applied to the regular vertical edge kind, once the tip result was a mild horizontal or vertical edge, it is delivered $R_{i,j}$ with the weighted average of $\widehat{D}_{i,j}^{Hgr}$ and,$\widehat{D}_{i,j}^{Vgr}$ to determine the missing pixel. If the result was no edge, then mean of $\widehat{D}_{i,j}^{Hgr}$ and $\widehat{D}_{i,j}^{Vgr}$ were used for interpolation. The equations are expressed as follows.

$$\widehat{G}_{ij} = R_{ij} + \widehat{D}_{i,j}^{W_{gr}} \qquad (11)$$

Where

$$\widehat{D}_{i,j}^{W_{gr}} = \begin{cases} \widehat{D}_{i,j}^{W_{gr}}, & if\ 4 \times \widehat{E}^{Hgr} \le \widehat{E}^{Vgr} \\ \left(3 \times \widehat{D}_{i,j}^{Hgr} + \widehat{D}_{i,j}^{Vgr}\right)/4, & if\ 2 \times \widehat{E}^{Hgr} \le \widehat{E}^{Vgr} < 4 \times \widehat{E}^{Hgr} \\ \widehat{D}_{i,j}^{V_{gr}}, & if\ 4 \times \widehat{E}^{Vgr} \le \widehat{E}^{Hgr} \\ \left(3 \times \widehat{D}_{i,j}^{Vgr} + \widehat{D}_{i,j}^{Hgr}\right)/4, & if\ 2 \times \widehat{E}^{Vgr} \le \widehat{E}^{Hgr} < 4 \times \widehat{E}^{Vgr} \\ \left(\widehat{D}_{i,j}^{Hgr} + \widehat{D}_{i,j}^{Vgr}\right)/2, & Othervise \end{cases} \qquad (12)$$

The missing of green channel in the B channel involved the same approach.

d) R-Plane and B-Plane Interpolator

The interpolation of the RI and bi was just like the delineated in Section C. within the Case 2, the equation of the interpolation of the missing blue channel within the R-channel is expressed as follows:

$$\widehat{B}_{i,j} = \widehat{G}_{ij} + \widehat{D}_{i,j}^{W_{gr}} \qquad (13)$$

$$\widehat{D}_{i,j}^{W_{gb}} = \begin{cases} \widehat{D}_{i,j}^{H_{gb}}, & if\ 4 \times \widehat{E}^{Hgb} \le \widehat{E}^{Vgb} \\ \left(3 \times \widehat{D}_{i,j}^{H_{gb}} + \widehat{D}_{i,j}^{V_{gb}}\right)/4, & if\ 2 \times \widehat{E}^{Hgb} \le \widehat{E}^{Vgb} < 4 \times \widehat{E}^{Hgb} \\ \widehat{D}_{i,j}^{V_{gb}}, & if\ 4 \times \widehat{E}^{Vgb} \le \widehat{E}^{Hgb} \\ \left(3 \times \widehat{D}_{i,j}^{V_{gb}} + \widehat{D}_{i,j}^{H_{gb}}\right)/4, & if\ 2 \times \widehat{E}^{Vgb} \le \widehat{E}^{Hgb} < 4 \times \widehat{E}^{Vgb} \\ \left(\widehat{D}_{i,j}^{H_{gb}} + \widehat{D}_{i,j}^{V_{gb}}\right)/2, & Otherwise \end{cases} \qquad (14)$$

The equation of the interpolation in the other cases are similar to the equation (13)-(14). After GI and RI & BI ona pixel. EODM can produce a full- colou pixel. With the completion of GI and RI&BI, a full- color image was obtained.

E). **Color interpolator**

Figure3.5 shows the two-stage pipeline design of the CI the sort choose (TS) module was used to choose the sort of edge, and the estimated difference calculator (EDC) was used to calculate the five possible color difference values of Dˆ_(i,j), as mentioned in (12) and (14) CI_1, CI_2, and CI_3 were used to catch the missing channel of $P_{i,j}$ for Case 1, 2, and 3, severally. As an example, CI_1 implements the equation (11) if the colour channel of $P_{i,j}$ is R channel. The implementation of CI_2 is comparable to that of CI_1. CI_3 requires the value $G^ˆ$ generated by CI_1. Figure8 shows the elaborate implementation of the TS module, within which the CMP is used to output Logic one if the higher input worth is larger than the lower worth. The combined unit was a priority encoder, and was used to mix the results of four CMPs to get a 3-bit worth. The elaborate implementation of module EDC is displayed in Figure9.

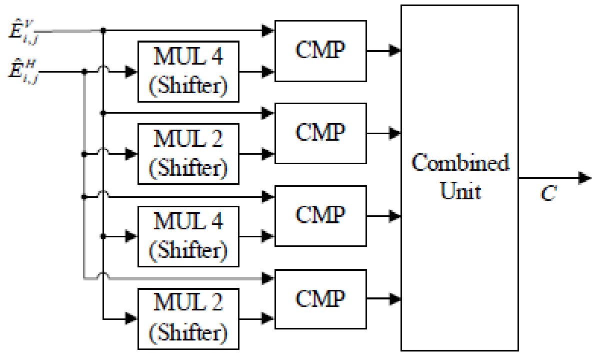

Figure8: TS Architecture

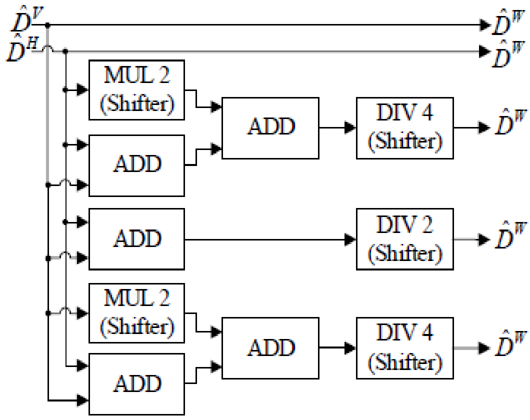

Figure9: EDC Architecture

ADVANTAGES:

- Low Cost
- Quality achievement of image.
- Only single CFA is required.
- Only one charge couple device sensor needed.
- No beam splitter is necessary.
- All color information is recorded at the same time.
- Camera is smaller and more economics.

APPLICATIONS:

- Image Processing applications.
- Computer Vision.

TABLE I
FIVE POSSIBLE VALUES OF *C* AND THEIR CORRESPONDING DIRECTIONS IN THE EODM.

Type	*C*	the chosen case
Normal Horizontal Edge	000	$if\ 4 \times \widehat{E}^{H_{OR}} \le \widehat{E}^{V_{OR}}$
Slight Horizontal Edge	001	$if\ 2 \times \widehat{E}^{H_{OR}} \le \widehat{E}^{V_{OR}} < 4 \times \widehat{E}^{H_{OR}}$
Normal Vertical Edge	010	$if\ 4 \times \widehat{E}^{V_{OR}} \le \widehat{E}^{H_{OR}}$

Slight Vertical Edge	011	$if\ 2 \times \hat{E}^{V_{OR}} \le \hat{E}^{H_{OR}} < 4 \times \hat{E}^{V_{OR}}$
No Edge	100	*Othervise*

V. IMPLEMENTAION RESULS, ANALYSIS AND COMPARISIONS

To verify the characteristics and quality of the demosaicked images obtained by using varied demosaicking algorithms, varied simulations were conducted on twenty four 512×768 Kodak images [24], and twelve globe images [25], like UHD (4096×2160) images, overexposed HD (1920×1080) images, and HD (1920×1080) images captured at low light levels. the photographs of the take a look at images are shown in Figure11. Many approaches were used to revive the analgesic CFA images. Thus, the rebuilt images were simply compared with the supply images for varied demosaicking ways. In this approach therefore by utterly reducing the buffer lines, hardware value, delay, and therefore image quality is increased. Figure 11, Figure12, Figure13, has showed several image pics of existing ones. Figure 14 showed the results of image with none contribution of buffer lines.

Figure11: Thirty six images for testing. initial six rows are 24 Kodak images, and therefore the different rows are designated UHD images, overexposed HD images, and HD images captured at low light levels.

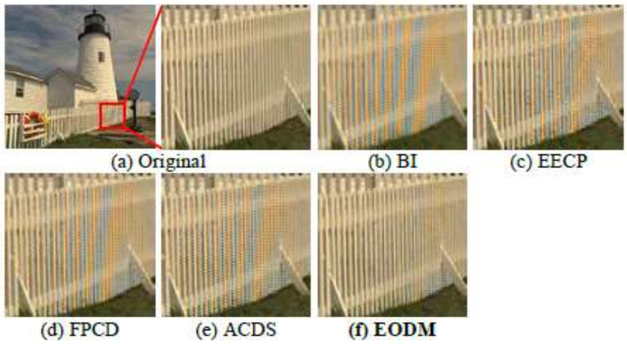

Figure 12: results of various low cost methods of restoring image 19.

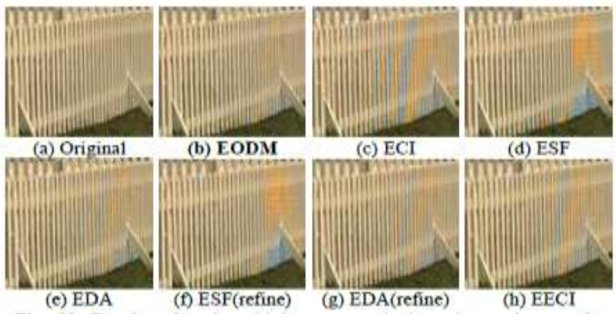

Figure 13: results of various higher-cost methods and ours in restoringimage19.

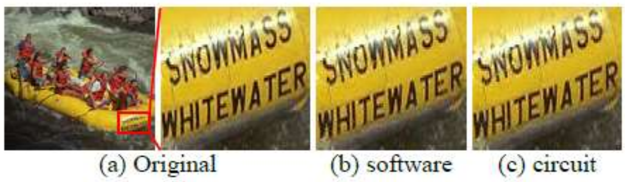

Figure 14: EODM results with software programme and VLSI circuit

Figure 15: Bayer CFA Image In

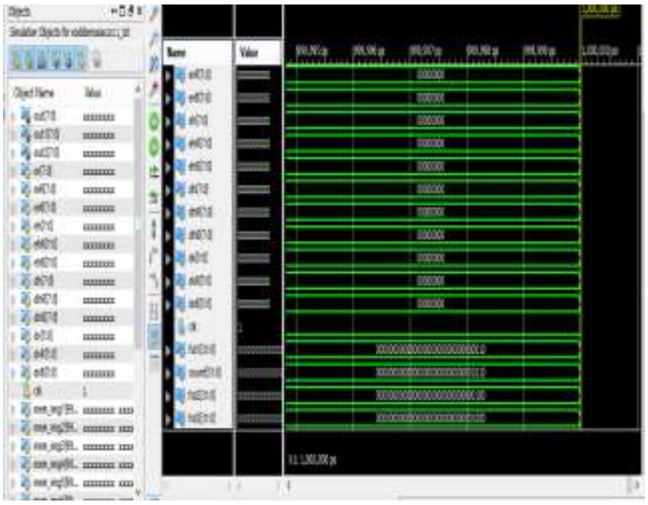

Figure 16: Simulation objects for eoddemosaic

TABLE II

COMPARISON OF CPSNR VALUES FOR VARIOUS DEMOSAICKING METHODS

method / images	LC					HC					
	BI[12]	EECP[14]	FPCD[15]	ACDS[16]	EODM	ECI[3]	ESF-R[5]	EDA-R[8]	ESF+R[5]	EDA+R[8]	EECI[10]
Image01	26.59	30.41	30.60	29.66	36.29	34.25	33.57	35.31	37.33	35.74	38.04
Image02	33.19	36.40	36.54	35.88	39.39	38.87	38.54	39.55	38.53	39.65	40.31
Image03	34.62	38.09	38.81	37.96	41.68	41.29	39.62	41.96	40.48	41.89	42.43
Image04	33.93	37.13	37.80	36.75	40.19	39.85	39.23	39.71	38.73	39.81	40.77
Image05	26.84	31.42	31.89	30.70	36.88	35.85	35.40	36.23	35.67	36.51	38.01
Image06	27.89	31.22	32.09	31.08	38.06	35.34	35.68	37.20	38.96	37.54	38.15
Image07	33.74	38.02	38.08	37.28	41.34	41.04	40.42	41.57	39.94	41.62	42.83
Image08	23.76	28.22	27.47	26.99	33.38	31.14	31.18	33.73	34.89	34.05	35.47
Image09	32.64	36.93	36.43	35.69	41.25	39.92	40.16	41.46	41.17	41.56	42.75
Image10	32.68	36.63	37.09	36.11	41.35	40.49	39.02	41.17	40.58	41.29	42.53
Image11	29.29	33.01	33.38	32.46	38.19	36.47	35.58	37.66	38.13	37.99	39.37
Image12	33.75	37.19	37.53	36.66	41.93	40.35	40.07	41.89	41.48	41.98	42.90
Image13	24.06	27.29	28.62	27.40	33.23	31.74	29.82	31.82	34.12	32.28	34.38
Image14	29.31	32.86	33.46	32.64	36.12	35.82	34.89	36.32	34.19	36.36	37.08
Image15	33.24	36.32	36.93	35.92	39.45	39.06	38.01	38.89	38.13	38.96	39.70
Image16	31.43	34.64	35.49	34.58	41.56	38.26	36.94	40.77	40.56	41.06	41.16
Image17	32.29	36.02	36.49	35.51	40.34	39.68	38.87	39.91	40.63	40.15	41.49
Image18	28.33	31.75	32.69	31.60	36.53	35.85	34.07	35.75	36.01	36.05	37.50
Image19	28.20	32.94	31.83	31.41	38.41	35.58	36.35	38.40	38.74	38.66	40.25
Image20	31.75	35.86	35.99	35.19	39.94	39.23	38.50	39.86	39.91	40.04	41.35
Image21	28.65	32.15	32.91	31.90	37.46	36.14	34.23	36.87	37.38	37.20	39.06
Image22	30.59	34.18	34.28	33.53	37.44	37.05	36.46	37.63	36.86	37.64	38.38
Image23	35.38	39.13	39.45	38.67	41.84	41.91	41.58	42.21	40.20	42.17	42.89
Image24	26.97	30.22	31.33	30.14	34.70	34.06	31.68	34.01	33.67	34.21	34.70
Image25	35.53	40.05	39.53	39.14	45.45	44.33	44.26	45.55	44.89	45.65	46.65
Image26	38.32	42.55	42.91	41.93	47.02	46.48	46.40	46.61	47.70	46.77	48.25
Image27	31.44	35.75	36.37	35.22	41.24	40.49	40.35	40.64	39.56	40.83	41.57
Image28	39.62	43.26	43.91	42.97	48.08	47.61	46.36	48.33	48.48	48.48	49.79
Image29	28.67	32.03	32.70	31.87	35.83	34.83	33.61	35.49	34.99	35.56	36.60
Image30	27.99	31.38	31.32	30.88	33.76	33.15	33.29	34.65	33.21	34.55	34.24
Image31	26.26	29.98	30.43	29.65	33.93	32.96	31.71	33.63	33.20	33.80	34.46
Image32	31.66	35.29	36.05	35.13	40.00	38.84	37.33	39.78	40.70	40.03	41.60
Image33	35.02	39.49	40.00	38.80	44.31	43.26	41.07	44.05	42.74	44.17	45.79
Image34	40.45	43.88	44.13	43.53	46.49	46.70	44.99	47.77	45.25	47.44	48.15
Image35	35.52	39.84	39.62	38.90	44.78	43.26	41.41	44.92	43.25	44.95	46.45
Image36	28.88	32.31	33.26	32.21	35.17	35.57	34.10	35.83	32.34	35.55	35.47
Ave	31.35	35.11	35.48	34.61	39.53	38.52	37.63	39.37	38.96	39.51	40.58

TABLE VII

FEATURES OF FOUR DEMOSAICKING IMPLEMENTATIONS.

	EECP[13]	FPCD[14]	ACDS[15]	EODM
ASIC Library(μm)	TSMC's 0.18	TSMC's 0.18	TSMC's 0.18	TSMC's 0.18
Line Buffer	2 lines	2 lines	2 lines	4 lines
Gate Counts	5.2K	4.97K	5.6K	21.08K
Frequency(MHZ)	200	200	200	200
Power(Mw)	4.66	4.76	150	106.8
Core area(μm²)	64.2K	60K	670K	224.2K
Quality	HD	HD	HD	HD
Throughput(pixel/s)	200M	200M	200M	200M

Figure 17: Edge oriented Demosaicked image

TABLE V

MASK SIZE AND LINE BUFFER OF EACH METHODS

method / type	LC					HC					
	BI[12]	EECP[14]	FPCD[15]	ACDS[16]	EODM	ECI[3]	ESF-R[5]	EDA-R[8]	ESF+R[5]	EDA+R[8]	EECI[10]
Mask Size	3×3	3×5	3×5	3×5	5×7	5×5	7×7	7×7	7×7	7×7	5×5
Line Buffer	3	2	2	2	4	8	11	9	15	13	25

LC = Lower-Cost HC = Higher-Cost −R = Without Refine +R = With Refine

TABLE VI

MEMORY GATE COUNTS OF THE REQUIRED LINE BUFFERING AT DIFFERENT RESOLUTIONS OF EACH METHODS

method / image size	LC					HC					
	BI[12]	EECP[14]	FPCD[15]	ACDS[16]	EODM	ECI[3]	ESF-R[5]	EDA-R[8]	ESF+R[5]	EDA+R[8]	EECI[10]
768×512	171.53K	114.48K	114.48K	114.48K	228.96K	514.55K	628.98K	514.55K	857.58K	743.18K	1429.73K
1920×1080	514.55K	345.36K	345.36K	345.36K	682.74K	1590.53K	1801.68K	1590.37K	2568.71K	2218.53K	4297.56K
4096×2160	1013.91K	675.93K	675.93K	675.93K	1351.96K	3041.13K	3716.74K	3041.13K	5068.13K	4392.39K	8446.78K

LC = Lower-Cost HC = Higher-Cost −R = Without Refine +R = With Refine

TABLE III

COMPARISON OF S-CIELAB VALUES FOR VARIOUS DEMOSAICKING METHODS

method / images	LC					HC					
	BI[12]	EECP[14]	FPCD[15]	ACDS[16]	EODM	ECI[3]	ESF-R[5]	EDA-R[8]	ESF+R[5]	EDA+R[8]	EECI[10]
Image01	4.88	3.38	3.50	3.69	1.81	2.17	2.17	1.90	1.54	1.74	1.47
Image02	3.00	2.29	2.33	2.38	1.69	1.73	1.71	1.57	1.66	1.55	1.46
Image03	1.71	1.28	1.27	1.29	0.92	0.95	0.99	0.86	0.97	0.88	0.85
Image04	2.35	1.79	1.76	1.85	1.29	1.29	1.33	1.29	1.34	1.29	1.16
Image05	5.43	3.75	3.84	4.09	2.13	2.38	2.32	2.20	2.38	2.08	1.85
Image06	3.53	2.43	2.43	2.46	1.23	1.60	1.40	1.29	1.12	1.21	1.18
Image07	2.02	1.44	1.52	1.56	1.07	1.11	1.07	1.00	1.25	1.01	0.91
Image08	5.59	3.85	4.27	4.47	2.01	2.59	2.39	2.00	1.76	1.84	1.63
Image09	1.76	1.26	1.35	1.41	0.86	0.94	0.85	0.80	0.82	0.80	0.74
Image10	1.74	1.27	1.30	1.37	0.86	0.89	0.93	0.83	0.87	0.82	0.74
Image11	3.63	2.63	2.71	2.79	1.59	1.88	1.79	1.58	1.44	1.50	1.32
Image12	1.42	1.05	1.07	1.09	0.70	0.77	0.73	0.66	0.69	0.67	0.62
Image13	6.85	5.00	4.66	5.02	2.77	3.04	3.53	3.00	2.51	2.76	2.36
Image14	3.93	2.80	2.76	2.83	1.78	1.92	1.96	1.78	1.95	1.74	1.62
Image15	2.45	1.93	1.93	2.03	1.46	1.41	1.47	1.41	1.52	1.45	1.28
Image16	2.72	1.91	1.91	1.91	1.01	1.34	1.30	1.04	1.02	1.00	1.01
Image17	2.68	2.05	2.06	2.14	1.45	1.47	1.52	1.43	1.37	1.39	1.26
Image18	4.74	3.49	3.35	3.60	2.21	2.27	2.57	2.29	2.56	2.22	2.04
Image19	3.41	2.37	2.52	2.64	1.36	1.65	1.52	1.40	1.24	1.32	1.16
Image20	2.10	1.56	1.59	1.66	1.03	1.10	1.13	1.02	1.02	1.00	0.90
Image21	3.32	2.40	2.35	2.46	1.42	1.59	1.76	1.49	1.35	1.38	1.20
Image22	2.77	2.05	2.05	2.18	1.43	1.44	1.49	1.39	1.61	1.42	1.30
Image23	1.40	1.12	1.13	1.16	0.93	0.91	0.89	0.87	1.08	0.89	0.86
Image24	3.44	2.43	2.42	2.61	1.50	1.60	1.79	1.51	1.58	1.47	1.32
Image25	1.92	1.34	1.43	1.38	0.80	0.91	0.75	0.80	0.75	0.80	0.70
Image26	1.30	0.95	0.96	0.93	0.63	0.70	0.58	0.62	0.57	0.64	0.55
Image27	2.93	2.03	2.07	2.13	1.29	1.43	1.22	1.32	1.42	1.33	1.23
Image28	1.18	0.93	0.92	0.89	0.68	0.72	0.63	0.60	0.62	0.66	0.56
Image29	1.96	1.37	1.34	1.41	0.87	0.98	1.03	0.92	0.95	0.93	0.79
Image30	1.90	1.30	1.37	1.37	0.97	1.09	0.97	0.92	1.02	0.94	0.91
Image31	2.46	1.70	1.70	1.77	1.06	1.21	1.27	1.12	1.11	1.07	0.96
Image32	1.02	0.69	0.69	0.70	0.46	0.52	0.50	0.46	0.47	0.46	0.40
Image33	1.86	1.47	1.43	1.43	1.06	1.16	1.10	1.02	1.12	1.13	0.97
Image34	1.49	1.27	1.23	1.20	1.09	1.13	0.99	0.90	1.08	1.06	0.91
Image35	2.34	1.89	1.91	1.86	1.30	1.50	1.36	1.24	1.37	1.43	1.22
Image36	3.41	2.74	2.71	2.74	2.27	2.34	2.28	2.05	2.64	2.31	2.06
Ave	2.80	2.03	2.05	2.12	1.30	1.44	1.43	1.29	1.33	1.28	1.15

CONCLUSION

This paper offers very sensible VLSI implementation for demosaicking. The intensive experimental results disclose that the planned layout achieved excellent performance in quantitative analysis and visual quality. For real-time applications, five-stage pipeline design was developed and applied for the EODM. The VLSI structure of the planned set up yielded a process rate of regarding 200 MP/s via the usage of the TSMC0.18-µm technology. For a 768×512 8-bit CFA check image, solely four lines (768×4×8 bits) had been needed for line buffering. Most advanced strategies buffer larger than eight lines. a number of them needed 25 strains for line buffering. Since the present sketch needed four lines for line buffering, it's terribly appropriate for various period functions within the planned style, the storage was once cut by quite ninetieth by means that of completely doing away with the buffer traces and so prolong and worth is reduced. The long run works can focal point on up the process overall performance and growing the period video application that is appropriate for action cameras and wearable devices.

REFERENCES

[1] B. E. Bayer, "Color imaging array," U.S. Patent 3 971 065, Jul. 1976.

[2] B. K. Gunturk, J. Glotzbach, Y. Altunbasak, R. W. Schafer, and R. M. Mersereau, "Demosaicking: Color Filter Array Interpolation," *IEEE Signal Process Mag*, Jan. 2005.

[3] S. C. Pei and I. K. Tam, "Effective color interpolation in CCD color filter arrays using signal correlation," *IEEE Trans. Circuits Syst. Video Technol*., vol. 13, no. 6, pp. 503-513, Jun. 2003.

[4] Y. S. Huang and S. Y. Cheng, " An Effective Color-Difference-Based Demosaicking Method," *J. Mar. Sci. Technol.*, vol. 21, no. 6, pp. 623-630, 2013.

[5] I. Pekkucuksen and Y. Altunbasak, "Edge Strength Filter Based Color Filter Array Interpolation," *IEEE Trans. Image Process*, vol. 21, no. 1, pp. 393-397, Jan. 2012.

[6] X. Chen, G. Jeon and J. Jeong, "Voting-based directional interpolation method and its application to still color image demosaicking," *IEEE Trans. Circuits Syst. Video Technol.*, vol. 24, no. 2, pp. 255-262, Feb. 2014.

[7] I. Pekkucuksen and Y. Altunbasak, "Multiscale Gradients-Based Color Filter Array Interpolation," IEEE Trans. Image Process, vol. 22, no. 1, pp. 157-165, Jan. 2013.

[8] W.-J. Chen and P.-Y. Chang, "Effective demosaicking algorithm based on edge property for color filter arrays," Digit. Signal Process, vol. 22, no. 1, pp. 163-169, Jan. 2012.

[9] X. Chen, G. Jeon, J. Jeong and L. He, "Multi-Directional Weighted Interpolation and Refinement Method for Bayer Pattern CFA Demosaicking," IEEE Trans.
Circuits Syst. Video Technol., vol. 25, no. 8, pp. 1271-1282, Aug. 2015.

[10] L. Chang and Y. Tan, "Effective use of spatial and spectral correlations for color Filter Array Demosaicking," IEEE Trans. Consum. Electron., vol. 50, no. 1, pp. 355-365, Feb. 2004.

[11] K. H. Chung and Y. H. Chan, "Color Demosaicing Using Variance of Color Differences," IEEE Trans. Image Process, vol. 15, no. 10, pp. 2944-2955, Oct. 2006.

[12] R. Ramanath, W.E. Snyder, G.L. Bilbro, and W.A. Sander III, "Demosaicking methods for Bayer color arrays," J. Electron. Image, vol. 11, no. 3, pp. 306–315, Jul. 2002.

[13] S. L. Chen, H. R. Chang and T. L. Lin, “Ultra-low-cost color demosaicking VLSI design for real-time video applications,” Electron. Lett., vol. 50, no. 22, pp. 1585–1587, Oct. 2014.

[14] S. L. Chen and E. D. Ma, "VLSI Implementation of an Adaptive Edge-Enhanced Color Interpolation Processor for Real-Time Video Applications," IEEE Trans. Circuits Syst. Video Technol., vol. 24, no. 11, pp. 1982-1991, Nov. 2014